

MINERAL DETECTION WITH CURIOSITY CHEMCAM PASSIVE REFLECTANCE DATA J. F. Mustard¹, E. Das^{1,2} ¹Brown University, Department of Earth, Environmental, and Planetary Sciences, Providence, RI, (john_mustard@brown.edu) ²Stony Brook University, Department of Geosciences, Stony Brook, NY.

Introduction: Mineral detection using hyperspectral data is typically achieved through matching the position, strength and shape of diagnostic absorption bands of remotely acquired data with laboratory reference spectra. While successful on one level, presence/absence detections on the basis of band position alone fails to get the most possible information from these data. Specifically, these approaches do not do well: when multiple mineral phases are present in the same pixel, when important minerals are present at concentrations <15%, accommodating the spectral diversity of laboratory spectral libraries, and in the presence of instrumental and calibration artifacts and noise [1]. This can be particularly difficult when using data from the visible to near-infrared (VNIR) (0.4-1.1 μm) wavelengths on Mars where absorption due to the presence of fine-grained ferric oxide minerals are extremely strong and mask the presence of other materials.

In this analysis we apply Factor Analysis/Target Transformation[2], a novel big-data mineral detection method previously used with orbital CRISM data[3–5], to test for the presence of minerals along the Curiosity traverse in Gale Crater using ChemCam passive reflectance data[6,7]. These are particularly challenging data as there are few uniquely diagnostic absorption features in this wavelength range and due to the strong influence of ferric oxide absorptions arising from dust. Nevertheless, this is the first application of factor analysis/target transformation (FATT) to point spectra acquired from a rover platform to assess the capabilities of FATT to identify spectral properties from ChemCam data consistent with laboratory minerals.

Methods: ChemCam data, calibrated to reflectance by Jeff Johnson as part of a PDART, covering the first 2,075 sols of the MSL mission [8] were downloaded from the PDS Geosciencde node. From these data, only passive reflectance observations of geologic targets rocks, outcrops and soils were extracted for analysis.

The data were then put into three mission phases for analysis: Bagnold Dunes [9], Stimson and Murray/Vera Rubin Ridge. We used the target definition to select ChemCam spectra for rock or soil targets, including veins, drill holes and tailings and brushed sites. Each mission phase was analyzed separately and results were compared to related literature[9–11].

We used RELAB spectra from the CRISM spectral library as candidate target spectra. This included 49 oxide, 144 inosilicate, 107 nesosilicate, 128

phyllosilicate, 24 sulfate and 74 carbonate spectra. The spectral library was clipped and resampled to the wavelength range and spectral sampling of ChemCam passive reflectance data for accurate comparison.

The complete suite of spectra for each phase were then processed using the FA/TT that consists of two steps: 1) Factor analysis and 2) Target transformation. Factor analysis was first applied to the ChemCam data to generate a suite of eigenvectors determined from the covariance matrix using the HYSIME algorithm [12]. The first 8 eigenvectors were then used as inputs to the Target Transformation. This subset of the eigenvectors, explaining the most variance in the data, are linearly fit to a library spectrum of a mineral of interest (e.g.[1]). Goodness of fit determined by the Root Mean Square Error (RMSE) of the eigenvectors fit to the laboratory spectra is the first metric used to reject or provisionally accept a fit. We use an (RMSE) threshold of $< 10^{-5}$ in this analysis. The spectra that meet the first criteria are then inspected visually to assess the quality of the fit. A subset of these is then analyzed in detail. A positive fit suggests there is a good probability that a spectral signature comparable to the laboratory spectrum is a spectral component in the ChemCam observation.

Results: The three campaigns result in some very strong fits of the FATT method to laboratory spectra and the best laboratory-FATT fits change with the campaigns.

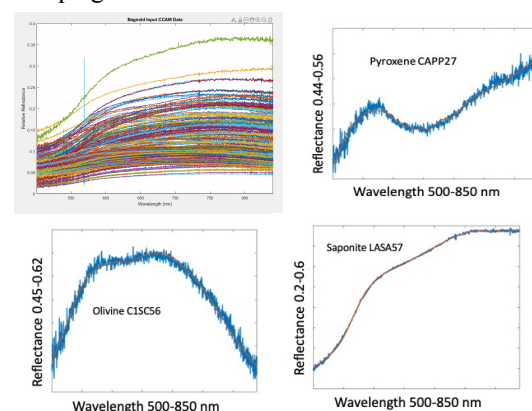


Figure 1: FATT fits to ChemCam spectra from the Bagnold Dunes campaign. The upper left shows all the input spectra, upper right shows a high quality fit to a pyroxene spectrum from the RELAB database with RELAB ID, lower left fit to an olivine spectrum from RELAB and lower right the fit to a saponite RELAB spectrum.

Figure 1 shows the fits to the ChemCam spectra from the Bagnold Dunes campaign. The quality of the fits are very good ($RMSE < 10^{-5}$). The example fits to the pyroxene and olivine show an envelope of stochastic noise that is quite a bit larger than for the saponite fit. This is likely due to the very different dynamic range of the laboratory spectra. The saponite spectrum has a dynamic range of 46% reflectance while only 12% and 17% for the pyroxene and olivine respectively. Both the pyroxene and olivine spectra show spectral features distinct from the typical ChemCam spectra in this suite.

There were a number of good fits to the Stimson campaign. However, in general the laboratory spectra that showed excellent fits were to materials that are not known to exist along the Curiosity traverse (e.g. [13]) such as diaspore. The laboratory spectra of these materials generally show a smooth spectrum rising from ≈ 400 nm to ≈ 750 nm, similar to the saponite example in Figure 1. Laboratory spectra with similar characteristics commonly results in fits that meet the RMSE threshold. We do not consider these types of fits to be compelling for followup.

FATT fits to the Upper Murray and Vera Rubin ridge campaigns show a new set of laboratory mineral spectra that provide excellent fits (Figure 2). Here we find iron oxides such as akaganeite, hematite and goethite easily meet the RMSE threshold. Furthermore, ChemMin analyses show that hematite and akaganeite are known to exist on Vera Rubin ridge [Rampe et al, 2019].

Discussion: Detailed spectroscopic analyses of ChemCam data in coordination with MastCam and mineralogic analyses have shown that absorption features and spectral parameters characteristic of mafic silicates (e.g. olivine) and iron oxides (e.g. hematite) are observed along the Curiosity traverse [9,10]. This pilot study applying the FATT method has shown that full spectral resolution characteristics of olivine, pyroxene, and iron oxides can be isolated from the ChemCam data. At the same time, we have found that many laboratory reflectance spectra show similarly high quality fits, like diaspore, but are likely not present on Mars and have not been detected by other approaches or in meteorites. False positives are a known limitation of FATT techniques [1].

We are now following up the more promising ChemCam detections to isolate the same features in ChemCam data not processed by factor analysis. Among the more interesting is the detection of goethite in the Vera Rubin ridge suite of ChemCam data (Figure 2). While this mineral was not detected in the ChemMin data (e.g. [13]) many alteration pathways to hematite include goethite as an intermediate step, which would inform the chemical conditions at the time of formation. Our work shows the robust applicability of FATT to

point spectrometer datasets and can be used to analyze future datasets to provide additional granularity in remote spectral compositional analyses. In the future, we will test out the approach on publically released SuperCam data obtained in the Jezero landing site using a broader wavelength region with more diagnostic absorptions.

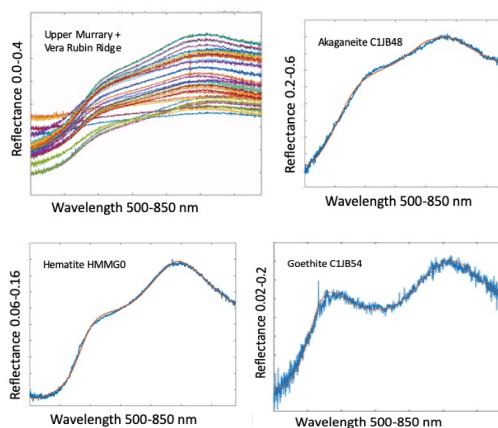


Figure 2: FATT fits to ChemCam spectra from the Upper Murray and Vera Rubin ridge campaign. The upper left shows all the input spectra, upper right shows a high quality fit to a akaganeite spectrum from the RELAB database with RELAB ID, lower left fit to an hematite spectrum from RELAB and lower right the fit to a goethite RELAB spectrum.

References: [1] Tarnas, J. D. et al. (2021) *Icarus*, 365, 114402. [2] Bandfield, J. L. et al. (2000) *J. Geophys. Res.*, 105, 9573–9587. [3] Thomas, N. H. and Bandfield, J. L. (2017) *Icarus*, 291, 124–135. [4] Tarnas, J. D. et al. (2019) *Geophysical Research Letters*, 46, 12771–12782. [5] Das, E. et al. *AGU Fall Meeting Abstracts*, (2020), pp. P038-07. [6] Wiens, R. C. et al. (2013) *Spectrochimica Acta Part B: Atomic Spectroscopy*, 82, 1–27. [7] Johnson, J. R. et al. (2016) *American Mineralogist*, 101, 1501–1514. [8] Johnson, J. R. et al. (2015) *Icarus*, 249, 74–92. [9] Johnson, J. R. et al. (2018) *Geophys. Res. Lett.*, 45, 9480–9487. [10] Jacob, S. R. et al. (2020) *J. Geophys. Res. Planets*, 125. [11] Horgan, B. H. N. et al. (2020) *J. Geophys. Res. Planets*, 125. [12] Bioucas-Dias, J. M. and Nascimento, J. M. P. (2008) *IEEE Trans. Geosci. Remote Sensing*, 46, 2435–2445. [13] Rampe, E. B. et al. (2020) *Geochemistry*, 80 25605.